

Proposal to PAC 53

Final-State Interactions Studies in Deuterium at Very High Missing Momenta

C. Yero[†] , P. Pokhrel, T. Horn, A. Singh, G. Kalicy, and Md. Hossain
The Catholic University of America, Washington, DC, USA

W. Boeglin*, **M. Sargsian[‡]**, H. Szumila-Vance, and G.P. Villegas
Florida International University, Miami, FL, USA

M.K. Jones*, J.O. Hansen, S.C. Dusa, T. Hague, and A. Tadepalli
Thomas Jefferson National Accelerator Facility, Newport News, VA, USA

S. Jeschonnek[‡]
The Ohio State University, Lima, OH, USA

E. Long and N. Santiesteban
University of New Hampshire, Durham, NH, USA

D. Nguyen
The University of Tennessee, Knoxville, TN, USA

S. Li, P. Datta, and J. Arrington
Lawrence Berkeley National Laboratory, Berkeley, CA, USA

H. Atac
Temple University, Philadelphia, PA, USA

N. Kalantarians
Virginia Union University, Richmond, VA, USA

E. Brash

Christopher Newport University, Newport News, VA, USA

M. Elaasar

Southern University at New Orleans, New Orleans, LA, USA

H. Mkrtchyan, A. Mkrtchyan, V. Tadevosyan, and A. Hoghmrtsyan

*A. I. Alikhanyan National Science Laboratory (Yerevan Physics Institute),
Yerevan, Armenia*

S. Bhattacharai

Idaho State University, Pocatello, ID, USA

E.R. Kinnery

University of Colorado, Boulder, CO, USA

D.L. Adhikari

Virginia Institute of Technology, Blacksburg, VA, USA

D. Bhesha and H. Bhatt

Mississippi State University, Mississippi State, MS, USA

C. Paudel

New Mexico State University, Las Cruces, NM, USA

Md. Junaid

University of Regina, Regina, SK, Canada

July 3, 2025

[†]Contact-spokesperson (yero@cua.edu), *Co-spokesperson, [‡]Theory Collaborator

Executive Summary

One of the unresolved problems of strong interaction physics is the understanding of QCD dynamics of nuclear forces at short distances. Progress in this direction is essential for understanding the dynamics of short-range correlations in nuclei as well as superdense nuclear matter relevant to the cores of neutron stars. Significant progress was made during the past two decades in exploration of nucleon-nucleon (NN) systems up to relative momenta of 650 MeV/ c , indicating the absence of non-nucleonic components and dominance of tensor interaction. However beyond 650 MeV/ c , the region where one expects the emergence of nuclear repulsion and the onset of non-nucleonic components is practically unexplored.

The most direct way of probing the NN system at short distance is considering high- Q^2 $d(e, e' N_f) N_r$ electro-disintegration reaction at large missing momenta in which the plane wave impulse approximation (PWIA) has the same magnitude as the initial nucleon momentum (p_i) inside the deuteron. However, considerable final state interactions (FSI) between the outgoing nucleons can strongly alter the expected relation between missing and initial momenta. Thus to be able to reach the repulsive core domain and identify possible signatures of non-nucleonic components, reliable understanding of FSI is required. *The interest towards studies of FSI effects at very large missing momenta is motivated by the recent experimental observation of strong deviation of the measured deuteron momentum distribution (at fixed recoil angle) from the prediction based on deuteron wave function consisting of the pn component only. It is intriguing that this deviation happens at missing momenta of ~ 800 MeV/ c which kinematically corresponds to the threshold of $NN \rightarrow \Delta\Delta$ transition in the deuteron.*

The first high-momentum transfer ($Q^2 > 1$ (GeV/ c) 2) $d(e, e' p) n$ reaction was measured at Jefferson Lab at 6-GeV showing a strong angular dependence of FSI with respect to the neutron recoil angle (θ_{nq}) relative to the momentum transferred (\vec{q}) where FSI were found to be the strongest at $\theta_{nq} \sim 70^\circ$, while being significantly reduced at forward angles, $\theta_{nq} \sim 30 - 40^\circ$ for neutron recoil (“missing”) momenta up to $p_m \sim 550$ MeV/ c . However, no data that studies this angular dependence currently exists above $p_m \sim 550$ MeV/ c , where one expects the emergence of nuclear core effects and where the above mentioned deviation is observed.

We propose to measure the $d(e, e' p) n$ reaction in Hall C with a 10.55-GeV electron beam incident on a 10-cm long liquid deuterium target. The scattered electrons will be detected by the Super High Momentum Spectrometer (SHMS) in coincidence with the knocked-out protons detected by the High Momentum Spectrometer (HMS), and the recoil (“missing”) neutrons will be reconstructed from momentum conservation. We will focus on the high missing momentum region of $p_m = 800$ MeV/ c and measure the unpolarized absolute cross sections for three central recoil angles: $\theta_{nq} = 49^\circ, 60^\circ, 72^\circ$ at $Q^2 = 4.5$ (GeV/ c) 2 .

Comparing the measured angular distributions to different theoretical models with FSI and relativistic effects which successfully describe $p_m \leq 550$ MeV/ c data we aim at establishing if the above mentioned deviation is due to FSI or represents the genuine property of the deuteron wave function. *If it is due to the wave function then this experiment for the first time will establish the existence of non-nucleonic components in the deuteron.*

This experiment was initially proposed to the Program Advisory Committee PAC 52 as the Letter-of-Intent LOI 12-24-005 (see the Appendix for our response to the questions raised in the PAC 52 comments). We request a total of 548 hrs (23 PAC days) which consists of 540 hrs of physics production and 8 hrs reserved for overhead. This work will be one of the first dedicated investigations of the dynamics of the NN repulsive core.

Contents

1 Physics Motivation	5
2 Theoretical Background	10
2.1 The Modern View of the Deuteron	10
2.2 Basic Diagrams and Kinematic Definitions of the Exclusive Reaction	11
2.3 Probing High Momentum pn and Non-Nucleonic Components in the Deuteron	12
2.3.1 High Momentum pn Component	12
2.3.2 Non-Nucleonic Components in the Deuteron	14
2.4 Theoretical Support for Deuteron FSI Studies	14
3 Experimental Program	15
3.1 Experimental Method	17
3.2 Simulations	17
3.2.1 Kinematic Coverage	20
3.2.2 Acceptance	23
3.3 Projected Statistical Results	24
3.4 Systematic Uncertainties	27
4 Beamtime Request	28
5 Summary	29
6 Appendix	33
6.1 PAC 52: LOI 12-24-005 Reader Comments	33
6.1.1 Question 1:	34
6.1.2 Question 2:	34

1 Physics Motivation

The deuteron is the most simple bound structure in nuclear physics and is therefore the “ideal laboratory” to study the nuclear short-range interaction. More specifically, when protons and neutrons come in close proximity, at extremely short distances ($\lesssim 0.8$ Fm) they experience a very strong repulsive force that keeps atomic nuclei from collapsing. Unfortunately, not much progress has been made with respect to this aspect of the nuclear force from both the theoretical and experimental standpoint. From the experimental aspect, the limitations have been mainly the low incident electron energies that could not provide sufficient resolution to probe such short distances.

From the theoretical standpoint, the description of short range nuclear phenomena based on meson theory of strong interaction faced an apparent problem since size of exchanged mesons (like ω -mesons) that generate a repulsion is comparable with the distances of the NN interaction. In the case of effective theories of strong interaction the short-range interactions are described by contact terms thus making it impossible to explore the dynamical origin of the NN repulsive core.

The most direct way to probe the repulsive core in the deuteron is via the exclusive $d(e, e'p)$ reaction (see Fig.6). In such a reaction we can identify its final state precisely (hence, *exclusive*) and at high Q^2 select kinematics to emphasize quasi-elastic knockout of the proton (referred to as plane-wave impulse approximation or PWIA) without competing processes such as (i) neutron-proton re-scattering effects also referred to as final-state interactions (FSI), (ii) meson-exchange currents (MEC) where the virtual photon couples to the exchanged meson or (iii) nuclear excitation into a resonance state (isobar currents or IC), each of which would distort the relationship between the neutron recoil (“missing”) momentum, p_m , and the proton initial momentum, p_i . The relative internal momentum of the bound proton can then be inferred from the reconstructed p_m .

Previous deuteron electro-disintegration experiments carried out at $Q^2 < 1$ (GeV/c) 2 (see Sec.5 of Ref. [1]) have helped quantify the contributions from FSI, MEC and IC to the $d(e, e'p)$ cross sections and determine kinematics at which these processes are either suppressed (MEC, IC) or under control (FSI). At larger Q^2 , MEC and IC are expected to be suppressed at $Q^2 > 1$ (GeV/c) 2 , and by selecting Bjorken $x_{Bj} \equiv Q^2/2m_N\nu > 1$ (m_N is the nucleon (proton) mass and ν is the energy transferred) where the lower energy transferred (ν) part of the quasi-elastic peak is maximally away from the inelastic resonance production threshold. Even at $Q^2 > 1$ (GeV/c) 2 and $p_m \gtrsim 300$ MeV/c however, FSI are still the dominant contribution to the cross sections compared to the PWIA, therefore they must be studied more carefully.

Final-state interactions have been studied theoretically by several groups [2–9]. In particular, one of the most important results of these studies is described by the generalized eikonal approximation (GEA) initially developed in Refs. [3, 4]. The establishment of the eikonal regime at $Q^2 > 1$ (GeV/c) 2 is characterized by a very anisotropic angular distribution of the neutron recoil angles (θ_{nq}) relative to the 3-momentum transfers, \vec{q} , and it makes it possible to identify kinematics where FSI are mostly canceled (see Fig.1).

The conventional non-relativistic Glauber approximation [4, 10, 11], which considers the bound nucleons as stationary scatterers, predicts FSI to peak at $\theta_{nq} \sim 90^\circ$. The GEA, however, which accounts for relativistic effects, predicts FSI to peak at $\theta_{nq} \sim 70^\circ$ for $p_m \sim$

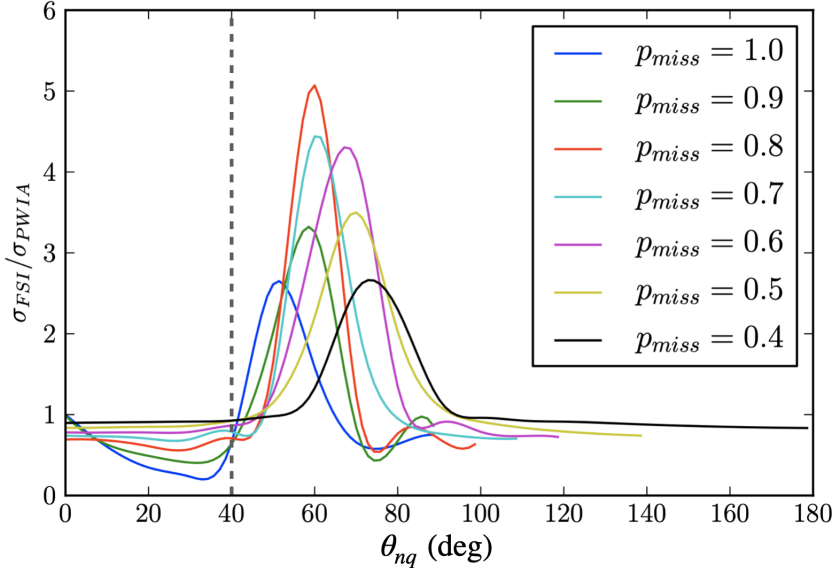


Figure 1: Ratios of the calculated FSI to PWIA cross sections (using the CD-Bonn potential) for different missing momenta as a function of the neutron recoil angle. Note: Reprinted from Ref. [1].

500 MeV/c. This prediction was confirmed by the first set of high- Q^2 deuteron electro-disintegration experiments carried out at Jefferson Lab [12, 13] (see Fig. 2). Additionally, it was also found that at very forward and backward neutron recoil angles of $\theta_{nq} \sim 40^\circ, 120^\circ$ FSI were significantly reduced and comparable to the PWIA. The reduction in FSI can be understood from the fact in the high energy limit ($Q^2 > 1$ (GeV/c) 2) of the GEA, the np re-scattering amplitude is mostly imaginary:

$$A = A_{\text{PWIA}} + iA_{\text{FSI}}, \quad (1)$$

with $A_{\text{FSI}} \approx i|A_{\text{FSI}}|$, where the total scattering amplitude A is expressed as the sum of the PWIA (A_{PWIA}) and the imaginary part of the FSI (A_{FSI}) scattering amplitudes. The total theoretical cross section can then be obtained by taking the modulus square of the total scattering amplitude and can be expressed as

$$\sigma_{\text{FSI}} \sim |A|^2 = |A_{\text{PWIA}}|^2 - 2\underbrace{|A_{\text{PWIA}}||A_{\text{FSI}}|}_{\text{"Screening" or interference term}} + \underbrace{|A_{\text{FSI}}|^2}_{\text{re-scattering term}}. \quad (2)$$

Taking the ratio of the total to the PWIA part of the cross section,

$$R = \frac{\sigma_{\text{FSI}}}{\sigma_{\text{PWIA}}} \approx 1 - 2\frac{|A_{\text{PWIA}}||A_{\text{FSI}}|}{|A_{\text{PWIA}}|^2} + \frac{|A_{\text{FSI}}|^2}{|A_{\text{PWIA}}|^2}. \quad (3)$$

From the ratio of cross sections the interference term enters with an opposite sign as compared to the re-scattering term, which provides an opportunity for an approximate cancellation at certain neutron recoil angles as shown in Figs. 1 and 2. This cancellation is also approximately independent of the neutron recoil momenta, which opens a kinematic window at

$\theta_{nq} \sim 40^\circ$ where one can probe the short-range structure of the deuteron beyond $p_m \sim 500$ MeV/c.

Another important feature of the GEA, and perhaps the one most relevant to this proposal is that the FSI peak, originally at $\theta_{nq} \sim 70^\circ$ for $p_m = 0.5$ GeV/c, shifts toward smaller recoil angles with increasing missing momenta as shown in Fig.1. This raises a very important question regarding the experimental sensitivity of the high-momentum component of the deuteron to FSI. In the most recent deuteron electro-disintegration experiment at Hall C [14], the internal momentum probed was extended up to $p_m \sim 940$ MeV/c (see Fig.3) at kinematics optimized for reducing FSI, based on the results from Ref. [12] (see Fig.2), by selecting central recoil angles $\theta_{nq} \sim 40^\circ$.

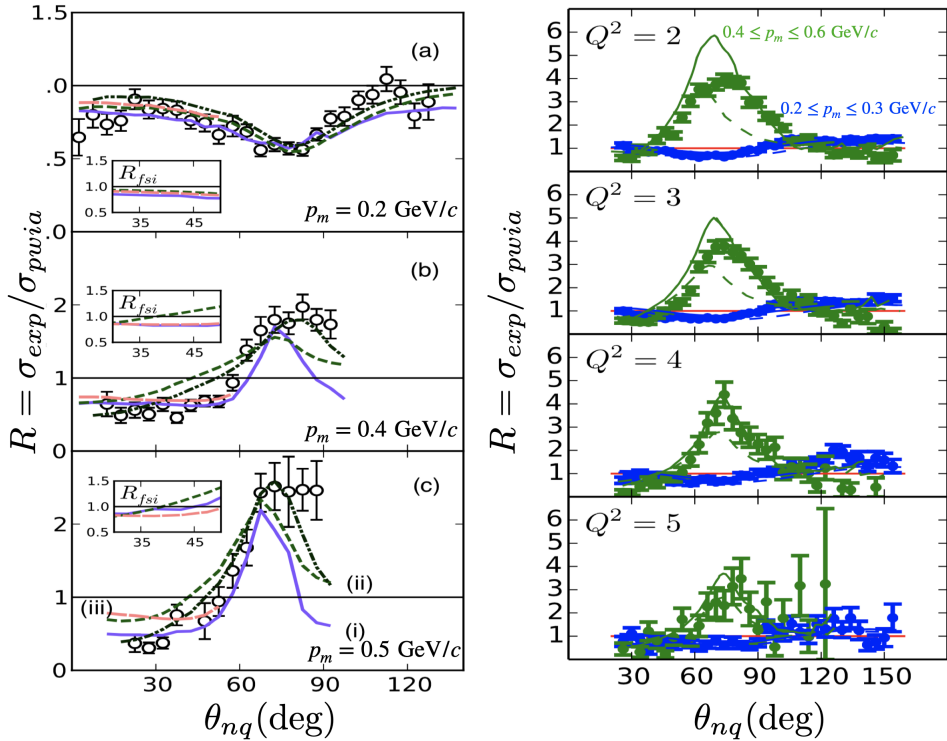


Figure 2: ${}^2\text{H}(e, e'p)n$ angular distributions of the cross section ratio, $R = \sigma_{exp}/\sigma_{pwia}$. (Left) Hall A data at $Q^2 = 3.5 \pm 0.25$ (GeV/c) 2 and missing momentum settings (a) $p_m = 0.2$ GeV/c, (b) $p_m = 0.4$ GeV/c and (c) $p_m = 0.5$ GeV/c. Theoretical calculations for (i) solid (purple) curves using the CD-Bonn potential by M. Sargsian [8], (ii) dashed (green) curves using FSI and dashed-double dotted (black) curves using FSI+MEC+IC by J.M. Laget [6] using the Paris potential and (iii) dashed (pink) curves denote calculations by J.W. Van Orden [7]. (Right) Hall B data at various Q^2 settings. The green data (with FSI re-scattering peak) correspond to $400 \leq p_m \leq 600$ MeV/c, and the blue data (no FSI re-scattering) correspond to $200 \leq p_m \leq 300$ MeV/c. The solid curves are calculations from J.M. Laget [6] and the dashed curves are from M. Sargsian [8]. Note: Reprinted from Ref. [1].

As shown in Fig.3, the data for up to $p_m \sim 650$ MeV/c agrees well with the previous Hall A measurements [12] and is reproduced by theoretical calculations that use the conventional deuteron wave function, consisting of only pn -component. However, **no theoretical model**

reproduces the data above $p_m \sim 750$ MeV/c. It is interesting that this disagreement appears at the momenta close to the kinematic threshold of $NN \rightarrow \Delta\Delta$ transition in the deuteron inelastic threshold momenta, $k_{inel} \sim \sqrt{M_\Delta^2 - M_N^2} \sim 800$ MeV/c.

It is interesting to note that recent theoretical calculations by Sargsian & Vera [15] (see Fig.4) using a relativistic deuteron wavefunction with explicit non-nucleonic component

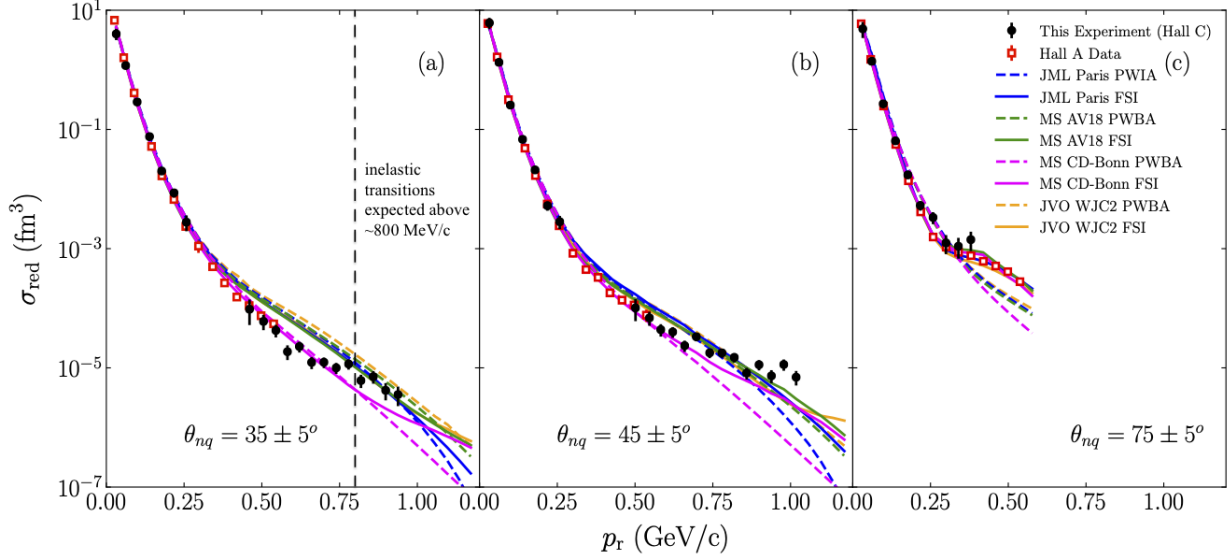


Figure 3: The experimental reduced cross sections (momentum distributions) for three values of the recoil angle θ_{nq} at $Q^2 = 4.5 \pm 0.5$ (GeV/c)² [14]. The solid lines are calculations including FSI and the dashed lines correspond to PWIA calculations [8].

starts to significantly deviate from the calculations which use the deuteron wavefunction with pn -component only, starting at internal momenta ~ 750 MeV/c which coincides with our published results (see Fig.3) from Ref. [14]).

Thus, the disagreement observed between the measurement and theory that used deuteron wavefunction with pn component only at $p_m \geq 750$ MeV/c, could be attributed to an enhanced role of the relativistic effects at higher internal momenta including inelastic transitions such as $\Delta\Delta \rightarrow np$ and $NN^* \rightarrow np$ as well as possible hidden color component in the deuteron near and above k_{inel} (see Sec.2 for details). To be able to disentangle relativistic effects from effects of non-nucleonic components in the deuteron wavefunction it was observed in Ref. [15] that non-nucleonic components violate so called “angular condition” which is satisfied by relativistic pn -component deuteron wavefunction, producing a specific angular distribution that can be measured experimentally.

Furthermore, from Eq.3 (see also Fig.3) one expects also a strong angular dependence of FSI effects. *Thus, to be able to verify an emergence of non-nucleonic components in the deuteron on needs a careful measurement of the angular distribution of the $d(e, e'p)n$ reaction at $p_m \gtrsim 800$ MeV/c. The theoretical analysis of the reaction based on pn relativistic wavefunction of the deuteron and FSI effects will allow us to verify the need of the non-nucleonic component in reproducing the strength and the angular distribution of the reaction.*

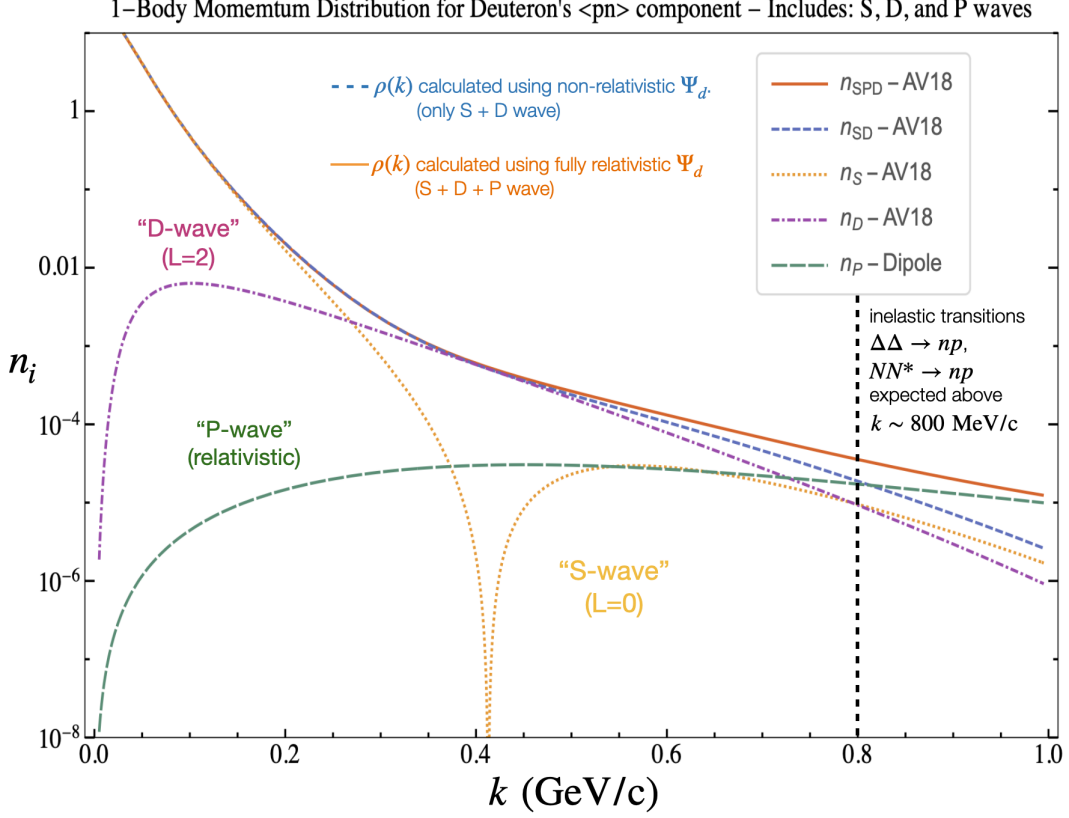


Figure 4: 1-body Momentum Distributions of the Deuteron using the AV18 potential. Reprinted from Ref. [16]

In this experimental proposal, our objective is to extend the angular distributions measured in Ref. [12] (see Fig.2 (left)) to a central missing momentum of $p_m = 800$ MeV/ c , a critical region corresponding to the repulsive core around which none of the deuteron models is able to reproduce the data in Fig.3. The proposed measurement will enable us to determine more precisely, the kinematic region where FSI are reduced, as well as separate the effects of FSI from possible contributions of non-nucleonic components of the deuteron [15], which are expected to show up around $p_m \sim 800$ MeV/ c .

2 Theoretical Background

2.1 The Modern View of the Deuteron

We start with decomposing the deuteron state vector into the Fock states restricted by the total spin, $J=1$ and isospin, $T=0$ quantum numbers of the deuteron:

$$\Psi_d = \Psi_{pn} + \Psi_{\Delta\Delta} + \Psi_{NN^*} + \Psi_{hc} + \Psi_{NN\pi} \dots \quad (4)$$

the “ \dots ”’s include the contributions from higher Fock components and higher mass constituents. In following we will discuss separately each component presented in Eq.(4).

pn Component: Kinematically one expects pionic degrees of freedom to become relevant at deuteron internal momenta exceeding ≈ 370 MeV/ c . However the empirical evidence suggests that the pn component is dominant for deuteron internal momenta up to 650 MeV/ c (see e.g. discussion in Ref. [17]). This can be understood based on the following facts: (i) the proportionality of the $N\pi N$ vertex to the pion momentum, (ii) the form factor of $N \rightarrow \pi N$ transition being hard $\sim \exp \lambda t$ with $\lambda \geq 3$ GeV $^{-2}$ [18] and (iii) the processes in which the high energy probe couples to the exchanged pion in the deuteron is significantly suppressed at high momentum transfer. These facts indicate that the dominant inelastic component can be the $\Delta\Delta$ rather than the $N\pi N$ component which will extend the pn dominance for up to $p_i \sim 800$ MeV/ c .

$\Delta\Delta$ Component: Due to the large cross section of the $\pi N \rightarrow \Delta$ transition and the above discussed suppression of the $N\pi N$ transition one expects the largest non-nucleonic component in the deuteron to be the $\Delta\Delta$ component. The current experimental constraints on the overall contribution of the $\Delta\Delta$ component is $\leq 1\%$.

NN^* Component: In principle the quantum numbers of the deuteron allow the NN^* component which will correspond to the radial excitation of one of the nucleons in the deuteron. Such an excitation will require a momentum of ~ 600 MeV/ c corresponding to internal momenta similar to the $\Delta\Delta$ component (~ 800 MeV/ c). However, empirically one expects a smaller $NN \rightarrow NN^*$ amplitude which may result in a contribution smaller than the contribution from the $\Delta\Delta$ component. Currently there is no experimental evidence or constraint on the possible mixture of the NN^* component.

Hidden Color Component: One of the unique predictions of QCD is the existence of the hidden color component in the deuteron wavefunction. In fact the color decomposition of a $6q$ system predicts almost 80% of the wavefunction strength to be due to the hidden color component [19, 20]. However one expects such a dominance only to occur at very large excitation energies of the NN system when the sum of the possible two-baryonic states in the deuteron is replaced by the six-quark representation. Since such large excitation energies are relevant to the nuclear core it raises an interesting possibility of the NN repulsive core being the result of the suppressed overlap between a hidden color-dominated configuration and the NN component.

$NN\pi$ Component: Finally, the most dominant three-particle Fock component of the deuteron is the $NN\pi$ component which one may expect to appear at excitation energies close to the pion threshold (corresponding to an internal momentum of ~ 370 MeV/ c) and

to be sensitive to the external probe at low momentum transfer. There is plenty of evidence of this component from low and intermediate energy reactions which probed meson exchange currents that start to dominate at the missing momentum range of ~ 350 MeV/c consistent with the above estimate of the pion threshold (see for example Refs. [21, 22]).

2.2 Basic Diagrams and Kinematic Definitions of the Exclusive Reaction

The most direct way of probing the internal structure of the deuteron is to study the exclusive

$$e + d \rightarrow e' + p + n \quad (5)$$

reaction in which one of the nucleons is struck by the incoming electron and the other is a spectator to the reaction.

We consider the reaction in which the detected nucleon in the final state of the reaction (Eq.5) is proton while the neutron is reconstructed through the energy-momentum conservation. We define the transferred four-momentum as (ν, \vec{q}) with a virtuality of $Q^2 = |\vec{q}|^2 - \nu^2$ and (E_f, \vec{p}_f) and (E_n, \vec{p}_n) as the four-momenta of the final proton and neutron respectively. We also define the missing momentum, p_m ,

$$-\vec{p}_m \equiv \vec{p}_i = \vec{p}_f - \vec{q} = -\vec{p}_n \quad (6)$$

which in the special case of direct PWIA (see Fig.5(a)) can be interpreted as a negative initial momentum vector of the bound proton which interacts with the electron.

Within the one-photon exchange approximation the basic Feynman diagrams that describe the exclusive process of Eq.(5) are given in Fig.5.

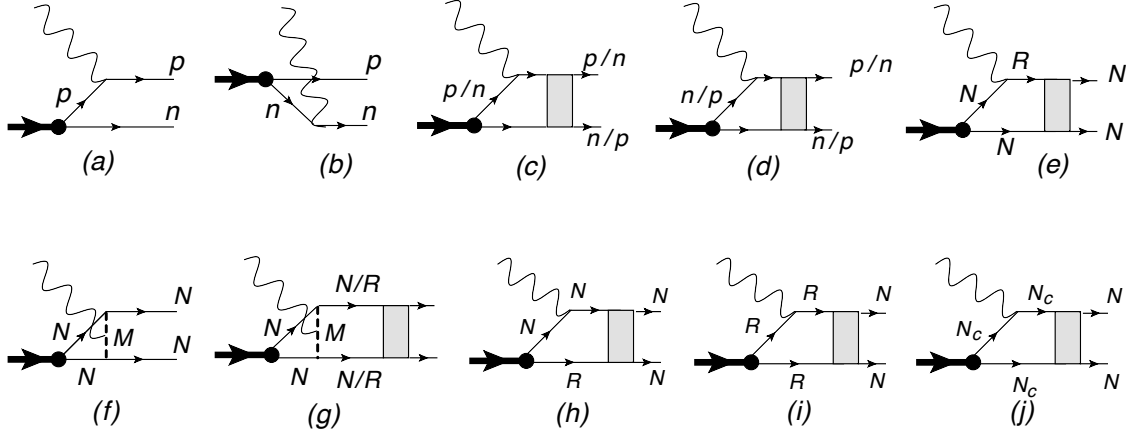


Figure 5: Diagrams contributing to the exclusive $d(e, e'p)n$ reaction.

These diagrams can be categorized as follows:

- (a) **Direct PWIA contribution:** We call the contribution of Fig.5(a) a direct plane-wave impulse approximation (PWIA) term, in which the detected nucleon (proton in the example) is knocked-out by the virtual photon while the undetected nucleon (neutron) is a spectator to the $\gamma^* p_{\text{bound}} \rightarrow p_{\text{final}}$ scattering. No final state interaction (FSI) is considered and therefore final nucleons emerge as plane waves.

- (b) **Spectator PWIA contribution:** In Fig.5(b) it is the undetected neutron which is struck by the virtual photon while the detected proton emerges as a spectator. Again no FSI is considered between the emerging nucleons.
- (c) **Direct FSI contribution:** In this case (Fig.5(c)) the struck proton rescatters off the spectator neutron and is detected in the final state.
- (d) **Charge-Interchange FSI contribution:** In this case (Fig.5(d)) the struck-nucleon undergoes a charge interchange interaction with the spectator nucleon.
- (e) **Intermediate State Resonance Production:** In Fig.5(e), the electromagnetic interaction excites the nucleon into a resonance state which then rescatters with the spectator nucleon into the final proton and neutron.
- (f) **Meson Exchange Contributions:** In Fig.5(f)-(g), the electromagnetic interaction takes places with the mesons which are exchanged between initial nucleons in the deuteron.
- (g) **Non-Nucleonic Contributions:** Final three terms contributing to the reaction (Figs.5 (h), (i) and (j)) are sensitive to the non-nucleonic component of the deuteron wavefunction. Here the first two represent the baryonic and the last, the hidden-color component contributions which was discussed in the Sec.2.

2.3 Probing High Momentum pn and Non-Nucleonic Components in the Deuteron

2.3.1 High Momentum pn Component

To probe the high momentum pn component of the deuteron in the diagrammatic presentation of the reaction (5), one needs to isolate the contribution from the direct PWIA process* (Fig.5(a)) at such momentum transfer \vec{q} and final proton momentum \vec{p}_f that the calculated missing momentum, according to Eq.6, is $p_m > 300 \text{ MeV}/c$. However such an isolation of high momentum pn component in the deuteron requires a suppression or reliable accounting for all the remaining contributions (diagrams Fig.5(b)-(j)) discussed in the previous section.

Our assertion is that this can be achieved if we consider the reaction (5) in *high-energy* kinematics in which the transferred momentum $q \geq \text{few GeV}/c$ and the virtuality of the probe, $Q^2 > 1 \text{ GeV}^2$, with an additional condition that the final nucleons (proton in our case) carries almost all the momentum of the virtual photon while the recoiling nucleon (neutron) is significantly less energetic, i.e.:

$$p_f \sim q \sim \text{few GeV}/c ; |p_m| = |\vec{q} - \vec{p}_f| \sim \text{few hundred MeV}/c ; Q^2 > 1 (\text{GeV}/c)^2. \quad (7)$$

The effects of the above conditions are different for different diagrams of Fig.5(b)-(j), which we can categorize as *kinematical*, *dynamical* and a mixture of both.

The suppression of the spectator PWIA diagram, Fig.5(b), is purely *kinematical*, since in this case the amplitude of the scattering will be defined by the deuteron wave function,

*Hereafter refereed as PWIA process.

$\sim \psi_d(p_i)$ with the initial momentum of $p_i \sim \text{few GeV}/c$ as compared to the PWIA term which is proportional to $\sim \psi_d(p_n)$ with $p_n \sim \text{few hundred MeV}/c$.

The diagrams containing meson exchange currents (Fig.5(f),(g)) will be suppressed *dynamically*, since in the limit of $Q^2 \gg m_{\text{meson}}^2 \sim 1 \text{GeV}^2$ they are suppressed compared to the PWIA term by an extra factor of Q^6 [23, 24]. Another dynamical suppression occurs in the scattering followed by the charge-interchange rescattering (Fig.5(d)). In this case the suppression is due to an extra $s^{-1/2}$ factor as well as a much stronger t dependence in the $pn \rightarrow np$ amplitude as compared to the $pn \rightarrow pn$ amplitude that enters in the direct FSI contribution (Fig.5(c)) [8]. For processes involving non-nucleonic components in the deuteron wavefunction (Fig.5(h-j)), one expects negligible contributions for up to $750 - 800 \text{ MeV}/c$ when approaching the inelastic threshold of $NN \rightarrow \Delta\Delta$ transition.

Finally, the suppression of processes involving intermediate baryonic resonance production (Fig.5(e)), which is expected to be large in the $\gamma N \rightarrow \Delta$ channel, is due to both kinematical and dynamical reasons. Kinematically, in the high energy limit it is possible to probe the lower (ν) side of the quasi-elastic peak (corresponding to Bjorken variable $x_{Bj} = \frac{Q^2}{2m_N\nu} > 1$) which is maximally away from the inelastic threshold of Δ electroproduction. Dynamically, due to the spin-flip nature of the $\gamma^* N \rightarrow \Delta$ transition one expects a much steeper falloff of the transition form-factor with Q^2 as compared to the elastic $\gamma^* N \rightarrow N$ scattering [25, 26].

The above discussion leaves us with the dominating contributions from the PWIA (Fig.5(a)) and direct FSI (Fig.5(c)* diagrams only. There is no obvious reason for the suppression of the latter diagram, since in the high energy limit the amplitude of $pn \rightarrow pn$ rescattering at small angles is dominated by the pomeron-exchange and is practically energy independent. However the most important change of the character of FSI in the high energy limit is the onset of the eikonal regime, in which case FSIs exhibit a strong angular anisotropy[†] being large at transverse and small at longitudinal directions of the recoil (slow) nucleon production.

Thus, we expect that in the high energy limit, defined according to Eq.7, the cross section of the process (5) will be defined mainly by the PWIA (Fig.5(a)) and FSI (Fig.5(c)) processes. In this case the concept of probing the high momentum component of the deuteron is related to measuring process (5) at large values of p_m which in the lab frame of the deuteron within PWIA corresponds to a large internal momentum in the deuteron. Such large missing momenta should be measured at forward or backward recoil nucleon angles which will minimize FSI effects allowing the direct access to the PWIA term.

The first comparisons of theoretical calculations based on the virtual-nucleon approximation (VNA) with experimental data demonstrated very reasonable agreement for up to $650 \text{ MeV}/c$ (Fig.3), of internal momenta indicating the full dominance of pn component in the deuteron. The VNA [8] is a relativistic approximation in which the spectator nucleon is treated on-shell and scattering nucleons energy is off-shell defined according to $E_i^{\text{off}} = M_d - E_s$, where M_d is the deuteron mass and $E_s \equiv \sqrt{m_n^2 + p_r^2}$ is the spectator (neutron) energy. The model uses a non-relativistic deuteron wavefunction minimally modified to account for baryonic number conservation.

*Referred hereafter as FSI diagram.

[†]This should be contrasted with the large and almost isotropic FSI at low and intermediate energies.

2.3.2 Non-Nucleonic Components in the Deuteron

To probe the non-nucleonic components in the deuteron we need to focus on kinematics which enhances contribution from diagrams of (Fig.5(h-j)). This can be achieved by measuring missing momenta above 800 MeV/c that corresponds to the threshold of $NN \rightarrow \Delta\Delta$ transition. An important issue in this case is how to separate relativistic effects in the pn -nucleonic system from non-nucleonic components in the deuteron.

The suggested approach is based on the observation that nucleonic and non-nucleonic components predict different angular distributions [15] for the reaction (5). This follows from the “angular condition” of the deuteron consisting only of the pn component, for which the unpolarized momentum distribution is independent on the angle of the internal momenta with respect to the \vec{q} . This condition is violated for the non-nucleonic components of the deuteron resulting in an angular dependence. The latter represents an experimental observable that can be used to identify non-nucleonic components in the deuteron.

2.4 Theoretical Support for Deuteron FSI Studies

Professor Misak Sargsian has been collaborating with us for many years. During this time, his contributions have been invaluable, and his publications relating to deuteron studies reflect the impact of this experiment to his work [1–4, 8, 15]. We have also formed a collaboration with Professor Sabine Jeschonnek, who has previous experience in exclusive electro-disintegration of both unpolarized and polarized deuterium [7, 27–30].

The endorsement of this proposal by both Drs. Sargsian and Jeschonnek will enable us to integrate current and future theoretical predictions from both frameworks. The following statement, for example, by Dr. Jeschonnek highlights the importance of the proposed experiment:

As stated in this proposal, gaining a better understanding of FSIs is very important for our ability to interpret experimental results in $(e,e'p)$ scattering. In Ref. [7], we introduced a calculation including all parts of the FSI – central, single spin-flip and double spin-flip, and avoiding unnecessary approximations like the assumption that the momentum transfer is transverse only. The latter approximation is good only for missing momenta less than 400 MeV/c. While many calculations include only the central part of FSIs, which is obviously the most important piece, the spin-dependent contributions can be sizable for some kinematics. This holds in particular for the peak region of the angular distributions. Therefore, the proposed experiment will be very helpful in better understanding FSI contributions.

3 Experimental Program

We propose to measure the $d(e, e'p)n$ absolute cross sections at $Q^2 = 4.5 \pm 0.5$ (GeV/c)² for 3 central recoil angles: $\theta_{nq} = 49^\circ, 60^\circ, 72^\circ$ corresponding to a central missing momentum setting of $p_m = 800$ MeV/ c . The selected recoil angles will provide a wide angular coverage to map out the FSI dependence on θ_{nq} . The angular distributions will be extracted by taking the ratio of the experimental cross sections to the PWIA theoretical cross sections versus neutron recoil angles, θ_{rq} . At such high Q^2 , it is expected that MEC and IC will have negligible contributions to the experimental cross sections for forward recoil angles. At larger angles ($\theta_{nq} > 70^\circ$), where $x_{Bj} < 1$, however, IC can still contribute significantly due to being near the inelastic electroproduction threshold, as evidenced by the data points in the last panel in Fig.2(left).

Measurements will also be done at $p_m = 500$ MeV/ c for $\theta_{nq} = 70^\circ$ at the same Q^2 . These data will be used for normalization measurements and comparison to the Hall A data [12]. In addition, we will also measure the ${}^1\text{H}(e, e'p)$ hydrogen elastic reaction to (i) check the spectrometer acceptance models, (ii) study target boiling effects and (iii) check systematic effects on beam energy and the spectrometer's central momentum and angle.

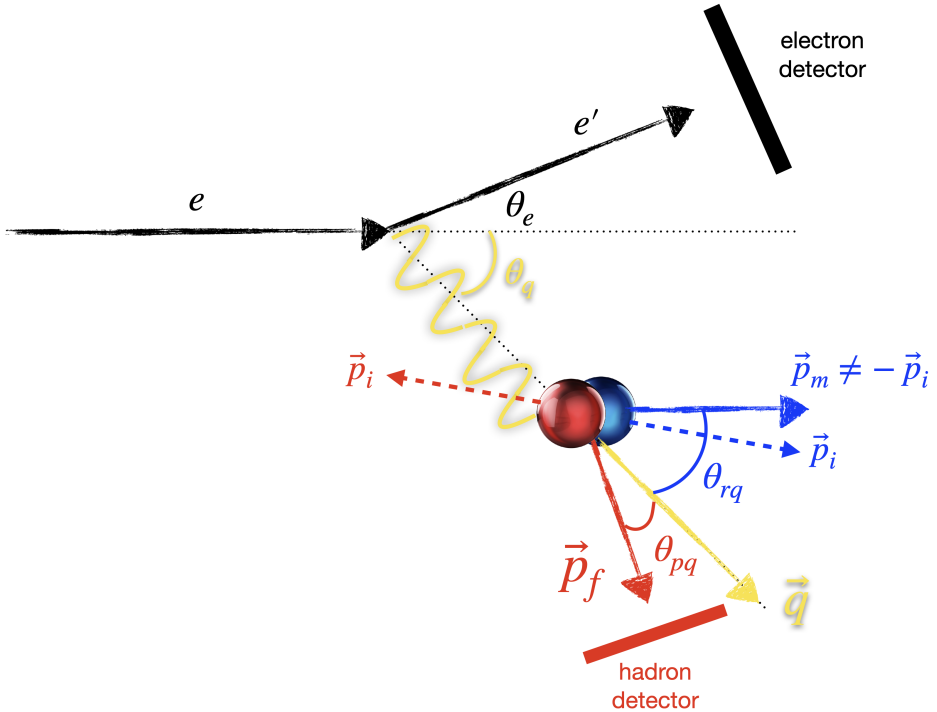


Figure 6: Schematic diagram of the $d(e, e'p)n$ reaction.

The experiment will be carried out at Jefferson Lab Hall C and will only require the standard experimental equipment. A 10.55-GeV, 3x3 mm² square-rastered electron beam will be incident on a 10-cm long liquid deuterium target. A typical $d(e, e'p)n$ reaction is shown in Fig.6 in which the incident electron interacts with the deuteron via the one-photon exchange approximation (OPEA), in which the scattered electron (k_f , θ_e) is detected by the Super High Momentum Spectrometer (SHMS) in coincidence with the

knocked-out proton (p_f , θ_p) detected by the High Momentum Spectrometer (HMS). The recoil neutron momenta (p_m) is reconstructed from momentum conservation. In Fig.6, the dashed vectors represent the relative internal momenta of the bound nucleons before interacting with the virtual photon. After the interaction, the bound proton is directly knocked-out, modifying its momentum. Within the PWIA, the spectator neutron would recoil with a missing momentum $\vec{p}_m = -\vec{p}_i$. However, due to FSI, the neutron re-interacts with the proton causing a modification in its recoil momentum such that $\vec{p}_m \neq -\vec{p}_i$. The modification of the neutron recoil momentum by FSI destroys any information related to the internal momentum of the deuteron. In either case, the modified missing momentum is determined by the vector difference $\vec{p}_m = \vec{q} - \vec{p}_f$, as shown in Fig.7. The central spectrometer kinematics are summarized in Table 1. A detailed description of the kinematics is covered in Section 3.2.1.

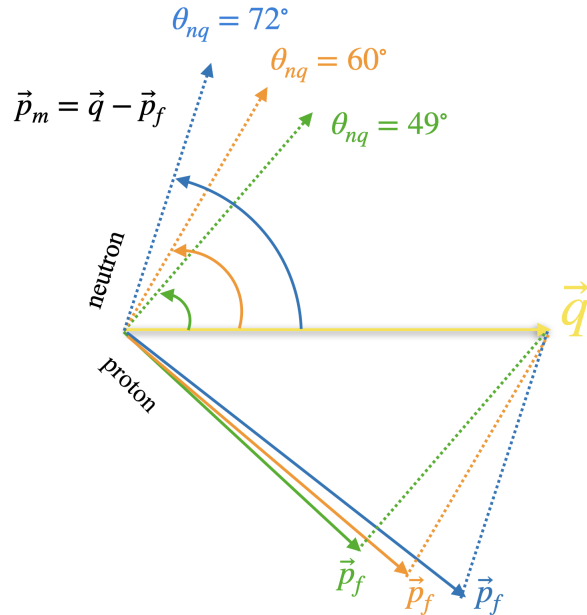


Figure 7: Schematic diagram showing the vector reconstruction of the recoil neutron \vec{p}_m from the virtual photon momentum transferred, \vec{q} , detected proton, p_f for each of the three central recoil angles, θ_{nq} . The dashed lines at the proton side are for reference.

p_m (MeV/c)	θ_{nq} (deg)	k_f (GeV/c)	θ_e (deg)	p_f (GeV/c)	θ_p (deg)
500	70	8.151	13.14	3.069	44.17
800	49	8.551	12.82	2.468	54.85
	60	8.151	13.14	2.891	49.27
	72	7.552	13.65	3.516	41.57

Table 1: Central spectrometer kinematics coverage for an incident electron beam energy of $E_b = 10.55$ GeV and $Q^2=4.5$ (GeV/c) 2 on a 10-cm liquid deuterium (LD2) target.

3.1 Experimental Method

Within the PWIA, the virtual photon couples directly to the bound proton, which is subsequently ejected from the deuteron without any further interaction with the recoiling neutron, the neutron carries a momentum equal in magnitude but opposite in direction to the initial momentum of the bound proton, $\vec{p}_m = -\vec{p}_i$, thus providing information on the momentum of the bound proton and its momentum distribution. However, if FSI are accounted for, the neutron momentum is modified by re-scattering with the knocked-out proton, and $\vec{p}_m \neq -\vec{p}_i$. For this specific case, assuming IC and MEC are negligible, one can still factorize the differential cross-section as follows:

$$\frac{d^6\sigma}{dE'd\Omega_e d\Omega_p dT_p} = K \cdot \sigma_{eN} \cdot S_D(\vec{p}_m \neq \vec{p}_i, E_m), \quad (8)$$

where K is a kinematic factor and σ_{eN} describes the elementary cross section for an electron scattering off a bound (off-shell) nucleon where the deForest [31] off-shell cross sections, σ_{cc1} or σ_{cc2} , are commonly used. The $S_D(\vec{p}_m, E_m)$ is referred to as a “distorted” spectral function, due to the modification of the recoil neutron momentum. In the approximation of $p_m \sim p_i$ (PWIA), the spectral function $S(\vec{p}_m \approx \vec{p}_i, E_m)$ would otherwise describes the probability of finding a bound proton with momentum \vec{p}_i and separation (“missing”) energy E_m .

We use the standard definition of missing energy: $E_{\text{miss}} = \nu - T_p - T_{\text{rec}}$, where ν is the energy transferred to the nucleus, and (T_p, T_{rec}) are the proton and recoil kinetic energies, respectively. For the special case of a deuteron break-up reaction, the recoil kinetic energy refers to that of the neutron. Since the deuteron has no excited states, the kinetic energies of the proton and neutron are well-defined and the missing energy becomes the binding energy of the deuteron, ~ 2.2 MeV. It follows that for the special case of the deuteron bound state, the separation (binding) energy can be integrated out of Eq. 8 to obtain,

$$\sigma_{\text{theory}} \equiv \frac{d^5\sigma_{\text{theory}}}{dE'd\Omega_e d\Omega_p} = K f_{\text{rec}} \sigma_{eN} S_D(\vec{p}_m), \quad (9)$$

where f_{rec} is the recoil factor that arises from the integration in E_m and is defined as [32]

$$f_{\text{rec}} \equiv \frac{1}{1 - \frac{1}{2} \frac{E_f}{E_r} \frac{q^2 - (p_f^2 + p_m^2)}{p_f^2}}. \quad (10)$$

where E_f is the final proton energy and E_r is the final neutron recoil energy (note this is different than E_m). From the experimental side, one can then take the ratio of the experimental cross sections to the theoretical cross sections only within the PWIA and bin the events in θ_{nq} to extract the angular distributions, similarly to the ones shown in Fig.2.

3.2 Simulations

The standard Hall C $A(e, e'p)$ coincidence simulation package (SIMC) was used to estimate the count rates for electron-scattering off a 10-cm long liquid deuterium target. The $d(e, e'p)n$ reaction was simulated for each of the central kinematics described in Table 1. The events were weighted by the theoretical model of the deuteron from J.M. Laget for both PWIA and

FSI (Paris NN potential) [6]. Furthermore, an efficiency factor based on the prior deuteron experiment [14] was also applied to the weight in order to account for experimental detector tracking inefficiencies in HMS/SMS (3% / 4%), data-acquisition dead-time (1%), target boiling effects (5%) and proton absorption (5%), which further reduced the yield in order to have a more conservative estimate.

additional simulation effects:

To have a more realistic estimate of the count rates, (i) *radiative* and (ii) *energy loss* effects were also included in the simulation. Radiative effects can significantly change the electron kinematics and therefore the measured yields. Energy loss effects account for the particles passage through the detector/spectrometer entrance and exit windows which also leads to a measurable effect in the yields.

event-selection cuts:

To select $d(e, e'p)$ coincidence events, we used the standard definition of missing energy in: $E_{\text{miss}} = \nu - T_p - T_{\text{rec}}$ previously defined in Section 3.1. Due to the finite energy resolution of the spectrometers, however, the binding energy of the deuteron is spread about its central value. In addition, spectrometer momentum ($\Delta P/P_0$) and angular acceptance cuts were also applied. The momentum acceptance refers to a relative variation of the detected particle momentum, ΔP , with respect to the spectrometer central momentum, P_0 . The angular acceptance refers to a relative variation in the scattered particles in-plane and out-of-plane angles with respect to the central spectrometer angle. The events are reconstructed and projected back to a collimator where the angular acceptance cut is applied. A summary of the cuts applied is presented in Table 2. The kinematics distributions are shown in 3.2.1.

analysis cut	range
E_{miss}	-20 to 40 MeV
Q^2	4 to 5 $(\text{GeV}/c)^2$
HMS $\Delta P/P_0$	-10 to 10 %
SHMS $\Delta P/P_0$	-10 to 22 %
HMS collimator	octagonal
SHMS collimator	octagonal

Table 2: SIMC event-selection cuts

background contributions:

From the previous $d(e, e'p)n$ coincidence experiment at Hall C [14], it was shown that the background sources were negligible as shown in Fig.8 (left) where the electron singles (SHMS), proton (HMS) singles and coincidence rates. The right panel of that same figure shows a typical coincidence time spectrum for the $p_m = 80$ MeV/c setting. Therefore, we

expect that the background contributions and trigger rates will not be a problem for the proposed experiment, which explores a similar region of missing momenta larger recoil angles ($\theta_{nq} \sim 49, 60, 72^\circ$) as compared to $\theta_{nq} \sim 40^\circ$ measured in Ref. [14].

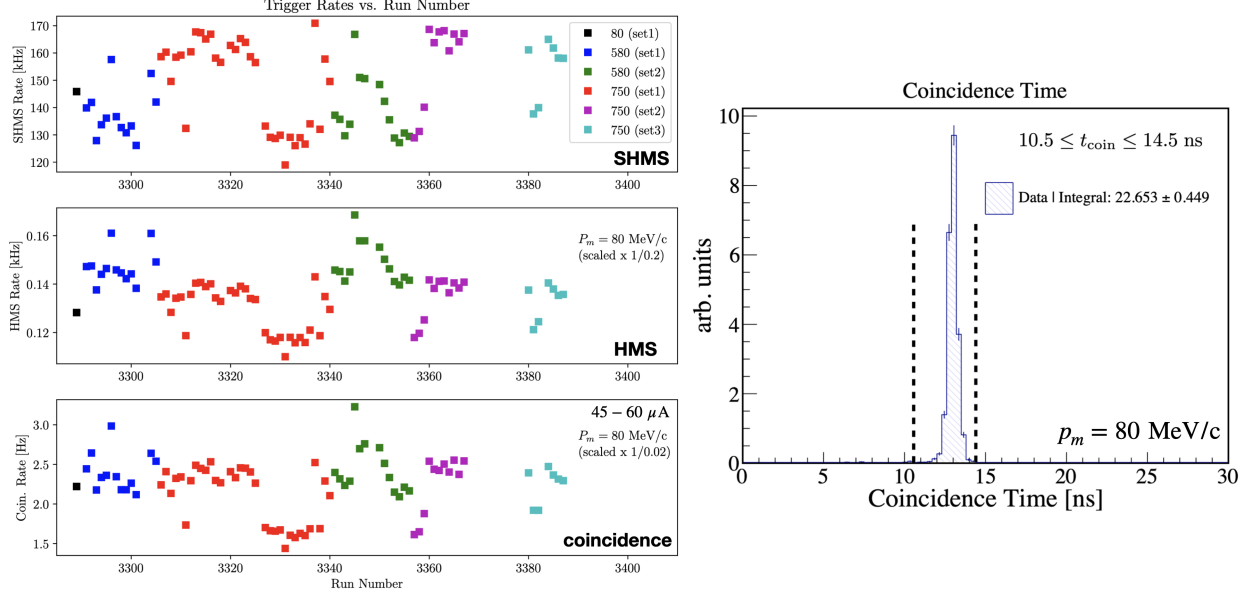


Figure 8: Trigger rates for the SHMS (top, in kHz), HMS (middle, in kHz) and coincidence trigger (bottom, in Hz) during the E12-10-003 experiment. Reprinted from Ref. [33].

count rate estimates:

p_m (MeV/c)	θ_{nq} (deg)	$d(e, e'p)$ rates (counts/hr)	DAQ rates (Hz)	beam-on-target (hrs)
500	70	456	0.467	12
800	49	41	0.0585	200
	60	105	0.101	144
	72	114	0.105	160

Table 3: $d(e, e'p)n$ rate estimates using the Laget FSI model with incident beam energy of 10.55 GeV at 80 μ A. Data-Acquisition (DAQ) rates exclude analysis cuts.

The following subsections show the relevant kinematic and acceptance variables with all event-selection cuts (Table2) and appropriately scaled by the beam-on-target.

3.2.1 Kinematic Coverage

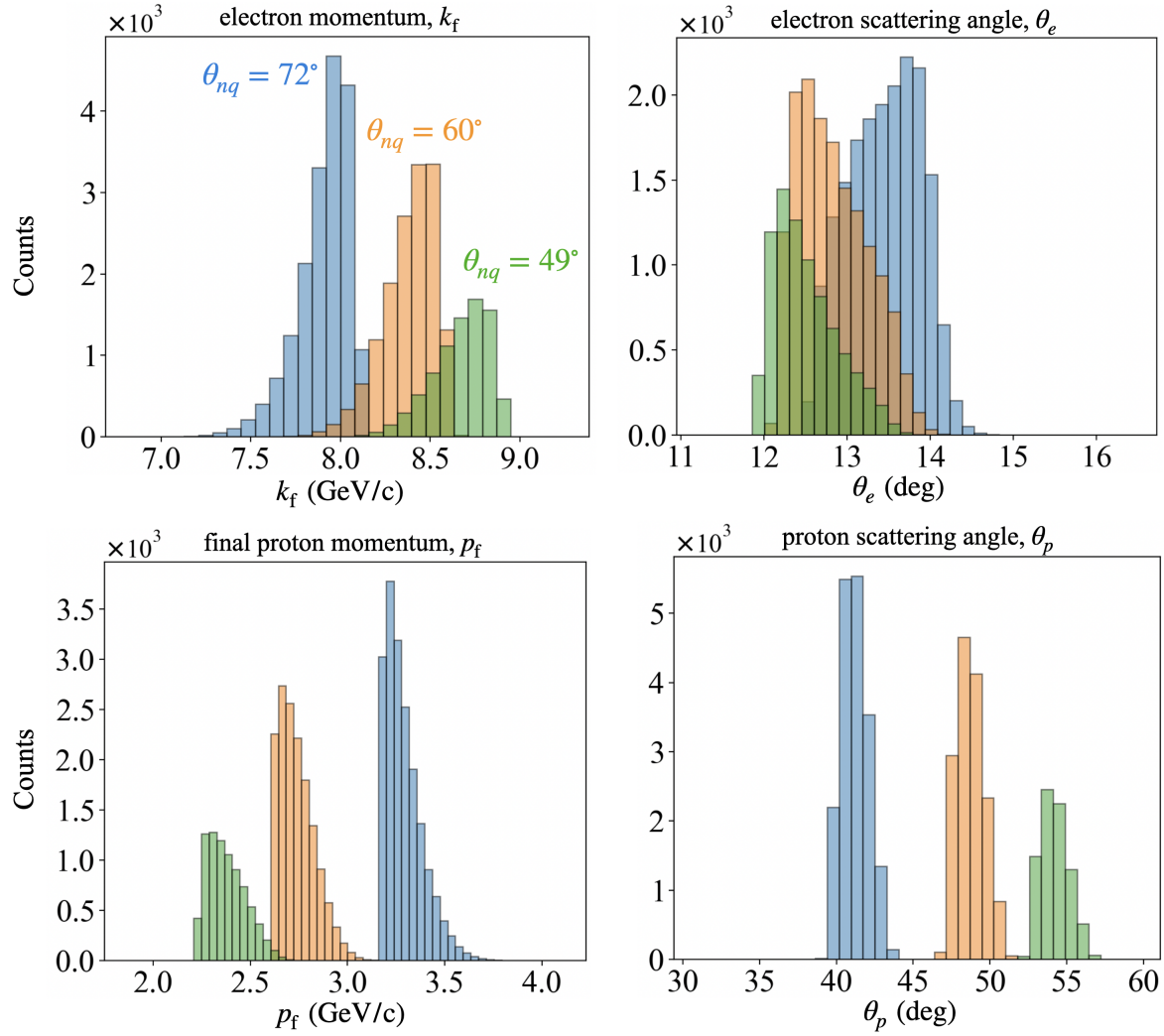


Figure 9: Simulated spectrometer kinematic distributions for SHMS (electrons) and HMS (protons) at $80 \mu\text{A}$.

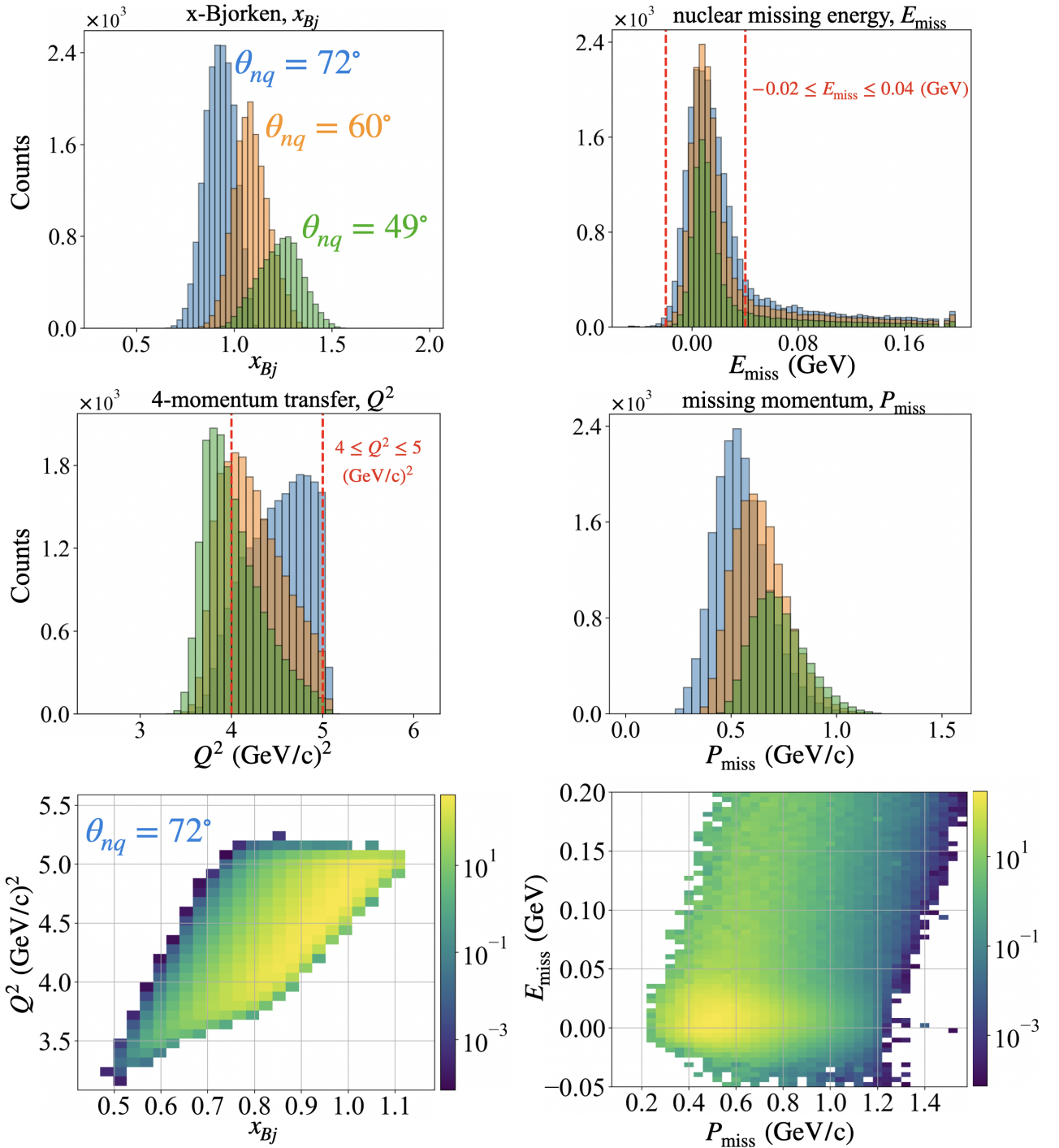


Figure 10: Additional kinematic distributions for x_{Bj} and Q^2 : (bottom 2 panels) 2D correlations of Q^2 vs. x_{Bj} (left) and E_{miss} vs. P_{miss} only for $\theta_{nq} = 72^\circ$. The color bar indicates the counts.

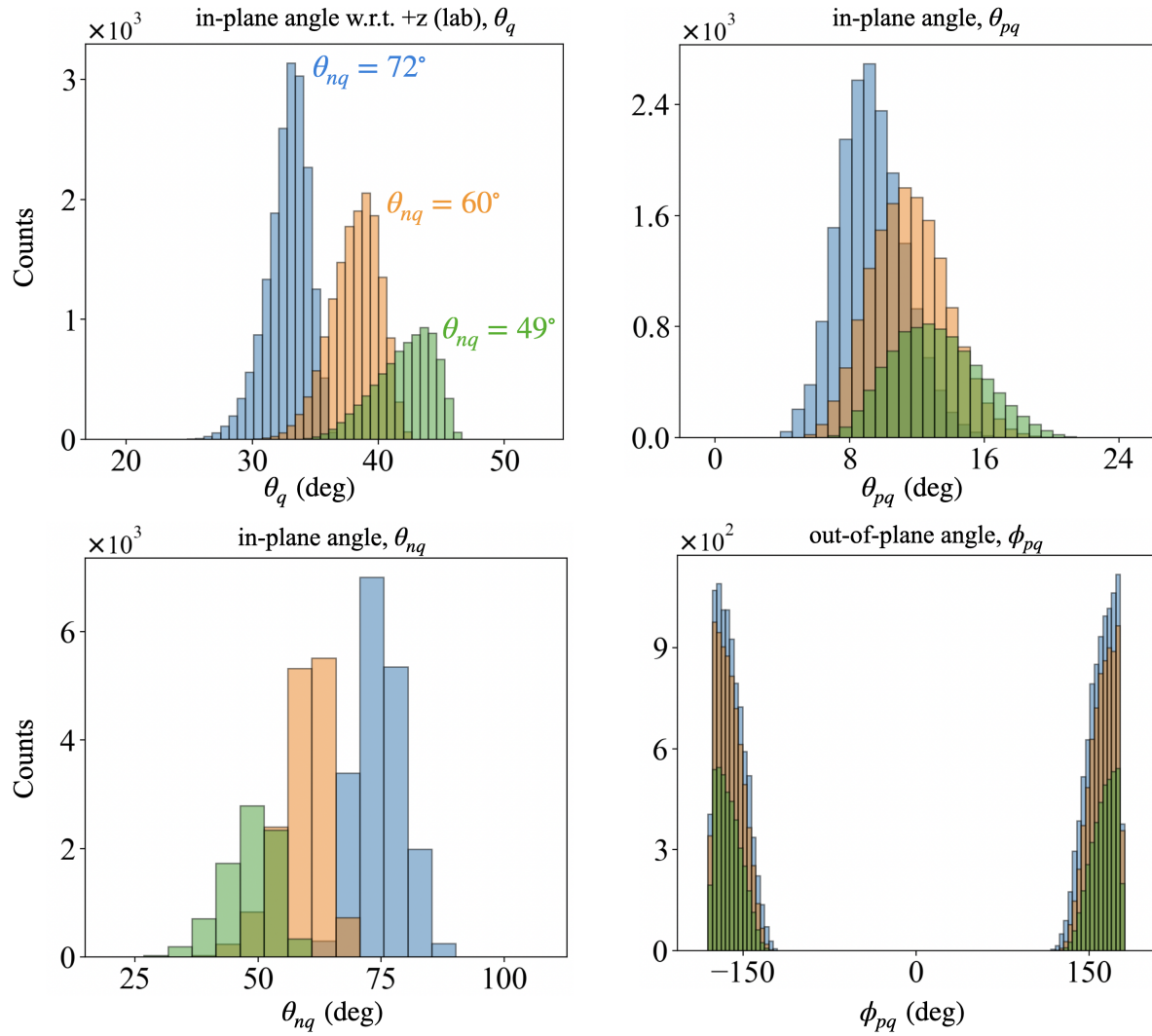


Figure 11: Angular kinematics showing the angles of \vec{q} and the angles of the proton and neutron relative to \vec{q} at $80 \mu\text{A}$.

3.2.2 Acceptance

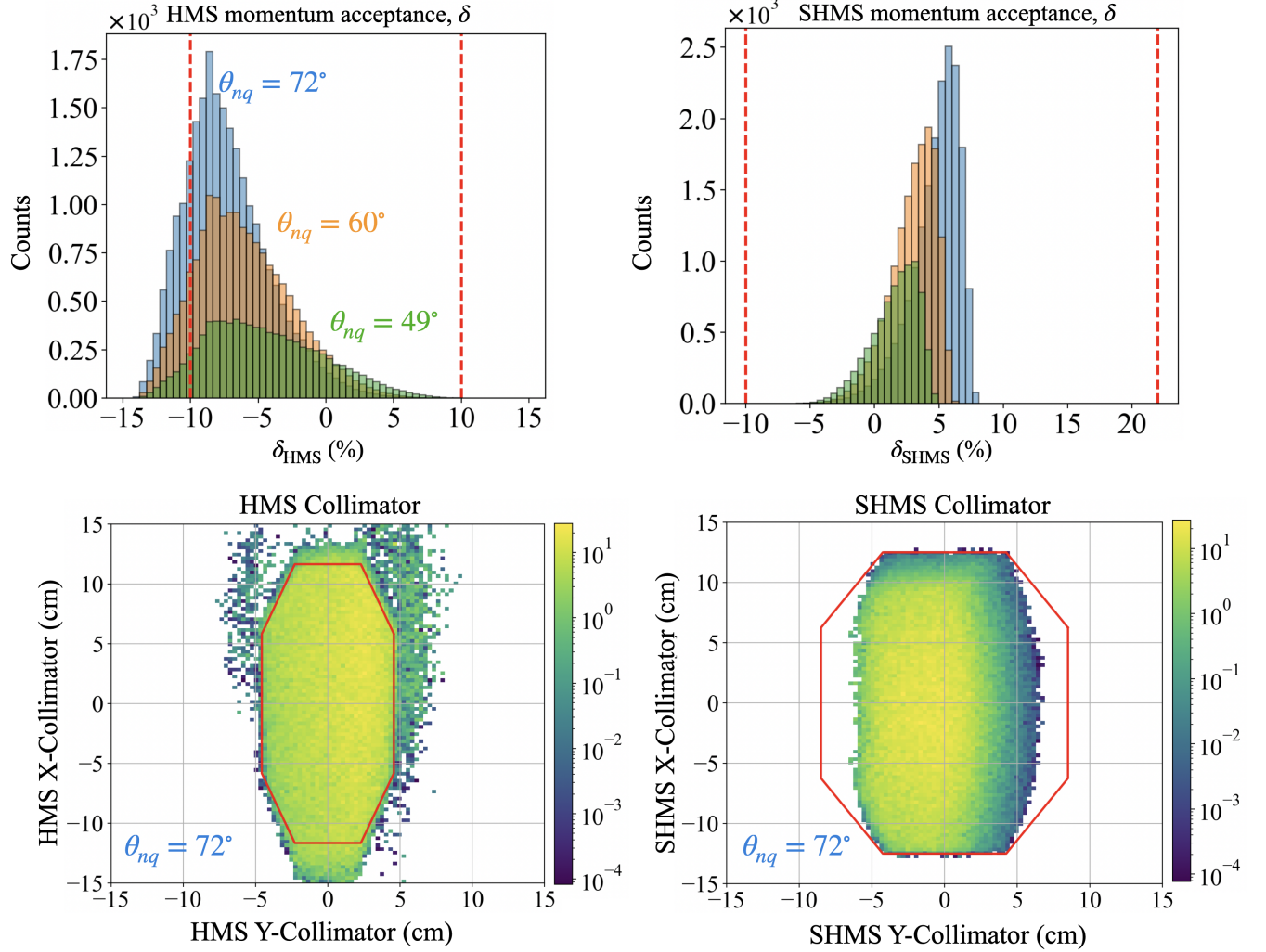


Figure 12: Momentum (top) and angular (bottom) acceptance distributions. The bottom panels show a contour line indicating the collimator geometry boundary; the HMS collimator determine the acceptance of the SHMS, as evidenced by most events in SHMS acceptance falling within the collimator geometry.

3.3 Projected Statistical Results

The simulation yield for both PWIA and FSI are binned in terms of $(p_{\text{miss}}, \theta_{nq})$ as shown Fig.13(top:FSI, bottom: PWIA). All analysis cuts summarized in Table2 have been applied.

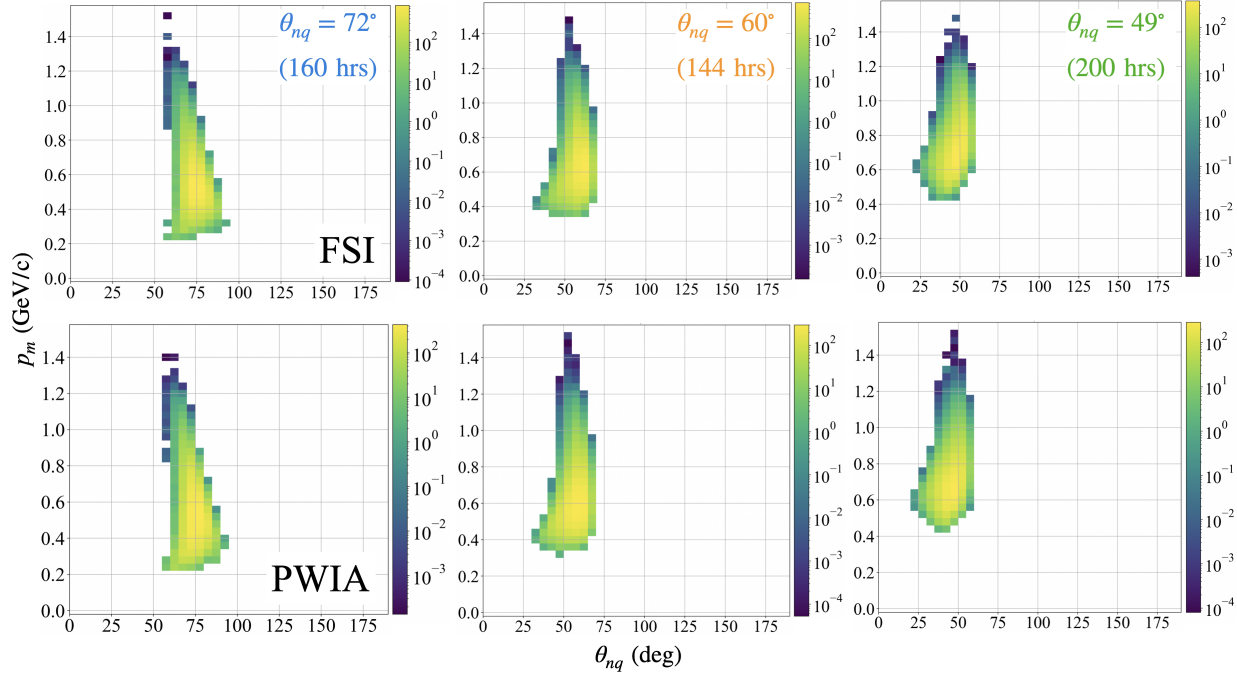


Figure 13: 2D correlation yield of p_{miss} vs. θ_{nq} for $\theta = 49, 60, 72^\circ$ using Laget FSI model [6].

To extract the angular distributions, the ratios of the 2D FSI to PWIA were taken for each (p_m, θ_{nq}) bin presented in Fig.13. The resulting ratio was then plotted versus θ_{nq} for different slices of p_m as shown in Fig.14. From the angular distributions, a FSI peak is clearly visible and starting at $\theta_{nq} = 70^\circ$ in the first p_m bin, and shows a gradual shift towards forward angles. One can also observe that the crossing at $\theta_{nq} \sim 40^\circ$, where the ratio is 1, is consistent throughout all the bins indicating the kinematic region where cancellation between the FSI and the PWIA/FSI interference term occurs, as was discussed earlier. These predictions have been experimentally verified for $p_m < 500$ MeV/ c , but will need to be verified for $p_m > 500$ MeV/ c , where relativistic effects play a more significant role. Furthermore, theoretical calculations that incorporate a relativistic deuteron wavefunction within the GEA framework are currently being developed by M. Sargsian using both the CD-Bonn and the AV18 potentials.

Figure 15 shows the projected statistical relative error on the FSI/PWIA ratios from Fig.14, where the red (dashed) lines used as a reference, represent the $\pm 20\%$ relative error mark, showing that most of the data points fall well within a statistical uncertainty of 20%.

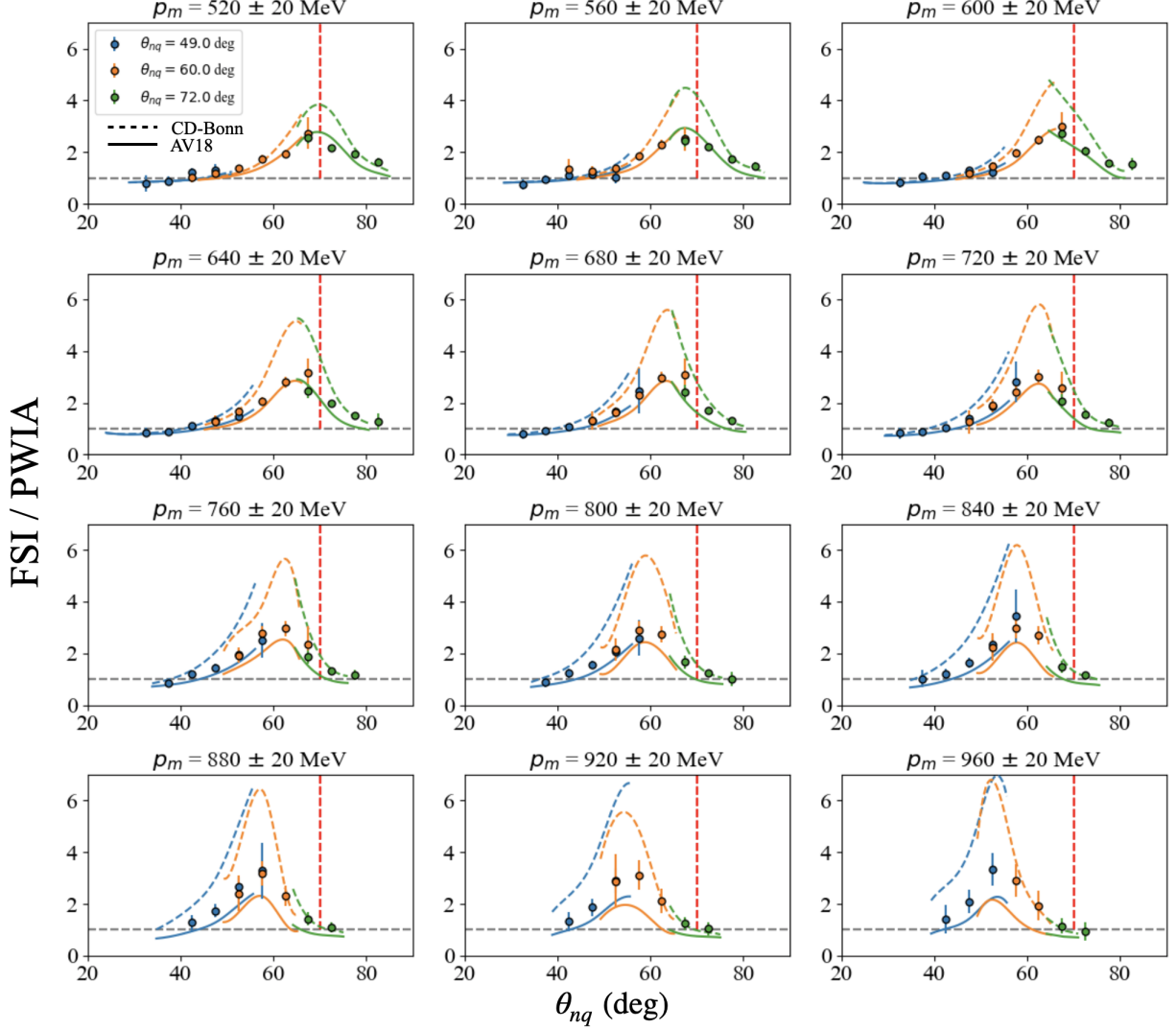


Figure 14: Angular distributions for θ_{nq} for $\theta = 49, 60, 72^\circ$ for a range of p_m bins using the Laget model (circles) of the deuteron. The dashed (CD-Bonn) and solid (AV18) theory curves are calculations using the virtual nucleon approximation (VNA) within the GEA framework by Sargsian [8]. The dashed (gray) horizontal line at 1 is used as a reference indicating no FSI. The dashed (red) vertical line is placed at $\theta_{nq} = 70^\circ$ for reference, to more easily observe the shift in the FSI peak.

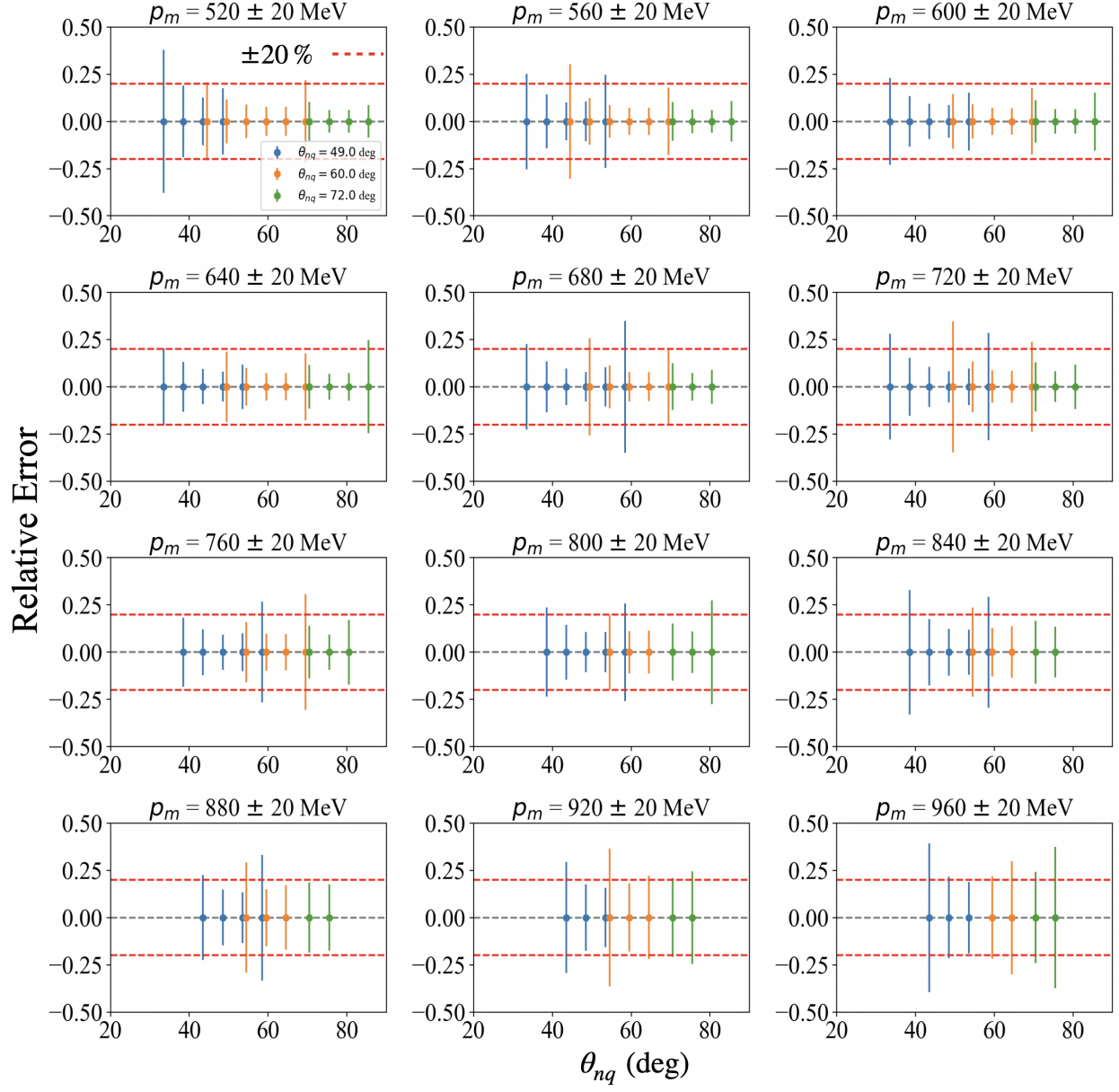


Figure 15: Relative error of angular distributions for θ_{nq} for $\theta = 49, 60, 72^\circ$ for a range of p_m bins using the Laget model of the deuteron. The dashed red lines indicate a $\pm 20\%$ relative error used as a reference.

3.4 Systematic Uncertainties

From the previous $d(e, e'p)$ measurements at Hall C [14, 33], which covered the range of missing momentum as that presented in this proposal, the major source of systematic uncertainties were well below 10%. There are two major sources of systematic uncertainties: (i) normalization, and (ii) kinematics.

The normalization uncertainties were typically on the order of 3 – 4% mainly due to the beam-current monitoring (BCM) calibration used in determining the charge normalization factor, the data acquisition dead time corrections as well as target boiling and proton absorption normalization corrections, as described in Ref. [33].

The kinematics uncertainties come mainly from the uncertainty in the determination of the incident beam energy as well as the spectrometers’ momentum and angle settings. These are usually determined by a series of dedicated hydrogen elastic data. From Ref. [14], these uncertainties were determined point-to-point in (p_m, θ_{nq}) bin and were added in quadrature for overlapping bins, with an overall kinematic uncertainty below 6.5%.

Given the similarity between the missing momentum range presented in this proposal and the commissioning deuteron experiment [14], we are confident that the overall systematic uncertainties will not go above 10%.

4 Beamtime Request

We propose a total of 548 hrs (\sim 23 PAC days) with 10.55-GeV beam energy, which consists of 540 hrs of physics production and 8 hrs of overhead. The overhead will be primarily allocated for the spectrometer momentum/angle changes between each of the central settings. Table 4 gives an overview of the time allocations for each part of the experiment.

From past experience on the data analysis of $d(e, e'p)$ at high missing momentum in Hall C [14,33], we estimate the singles rates of the experiment to be on the order of a few hundred kHz (for SHMS singles), a few hundred Hz (for HMS singles) and on the order of a few Hz for the coincidence trigger rates.

target	current (μA)	p_m (MeV/c)	θ_{nq} (deg)	data-taking (hrs)	overhead (hrs)
LD2	80	500	70	24	2
LD2	80	800	49	200	2
			60	144	2
			72	160	2
LH2	80	$^1\text{H}(e, e'p)$ elastic		8	
C12/LD2/LH2	10-80	target boiling		2	
no target	0-80	BCM calibration		2	
total				540	8
				(23 PAC days)	548 hrs

Table 4: Beam time allocation. The targets are defined as: 10-cm liquid deuterium (LD2), 10-cm liquid hydrogen (LH2), carbon-12 foil (C12).

5 Summary

In summary, this proposal aims to measure for the first time the angular (θ_{nq}) distributions of the FSI/PWIA cross-section ratios for the exclusive $d(e, e'p)n$ reaction at large momentum transfers ($Q^2 = 4.5 \text{ (GeV}/c)^2$ and very high missing momenta ($p_m \sim 800 \text{ MeV}/c$) which corresponds to a kinematic region where the non-nucleonic components of the deuteron are expected to become relevant [15].

The previous $d(e, e'p)$ commissioning experiment [14] at Hall C extended the missing momentum reach up to $940 \text{ MeV}/c$ optimized for kinematics with reduced FSI at forward angles $\theta_{nq} \sim 40^\circ$. The unexpected results of that experiment, particularly the deviations measured above $p_m \sim 800 \text{ MeV}/c$, which coincides with the theoretical expectation of the inelastic non-nucleonic $\Delta\Delta \rightarrow np$ transition within the deuteron [15], has reinvigorated a high theoretical as well as experimental interest in studying the nuclear repulsive core of this simple nucleus.

The main objective of this proposal is therefore to extract the FSI/PWIA angular distributions. By comparing the angular distributions to different theoretical models with FSI and relativistic effects, which successfully describe $p_m \leq 550 \text{ MeV}/c$ data, we will be able to determine whether the above-mentioned deviations at $p_m \sim 800 \text{ MeV}/c$ are due to FSI or represents the genuine properties of the deuteron wave function. If we find that FSI do not contribute to the deviations at high missing momenta observed in Ref. [14], then this experiment for the first time could establish the existence of non-nucleonic components in the deuteron.

References

- [1] W. Boeglin and M. Sargsian, *Modern studies of the Deuteron: From the lab frame to the light front*, *International Journal of Modern Physics E* **24** (2015) 1530003, [<https://doi.org/10.1142/S0218301315300039>].
- [2] L. L. Frankfurt, W. R. Greenberg, G. A. Miller, M. M. Sargsian and M. I. Strikman, *Color transparency effects in electron deuteron interactions at intermediate Q^{**2}* , *Z. Phys. A* **352** (1995) 97–113, [[nucl-th/9501009](#)].
- [3] L. L. Frankfurt, M. M. Sargsian and M. I. Strikman, *Feynman graphs and generalized eikonal approach to high energy knock-out processes*, *Phys. Rev. C* **56** (Aug, 1997) 1124–1137.
- [4] M. M. Sargsian, *Selected Topics in High Energy Semi-Exclusive Electro-Nuclear Reactions*, *International Journal of Modern Physics E* **10** (Dec, 2001) 405–457.
- [5] C. Ciofi degli Atti and L. P. Kaptari, *Calculations of the exclusive processes $H\text{-}2(e, e'\text{-prime } p)n$, $He\text{-}3(e, e'\text{-prime } p)H\text{-}2$ and $He\text{-}3(e, e'\text{-prime } p)(pn)$ within a generalized Glauber approach*, *Phys. Rev. C* **71** (2005) 024005, [[nucl-th/0407024](#)].
- [6] J. Laget, *The electro-disintegration of few body systems revisited*, *Physics Letters B* **609** (2005) 49 – 56.
- [7] S. Jeschonnek and J. W. Van Orden, *New calculation for $^2H(e, e'p)n$ at gev energies*, *Phys. Rev. C* **78** (Jul, 2008) 014007.
- [8] M. M. Sargsian, *Large Q^2 electrodisintegration of the deuteron in the virtual nucleon approximation*, *Phys. Rev. C* **82** (Jul, 2010) 014612.
- [9] W. P. Ford, S. Jeschonnek and J. W. Van Orden, *$^2H(e, e'p)$ observables using a Regge model parameterization of final state interactions*, *Phys. Rev. C* **87** (2013) 054006, [[1304.0647](#)].
- [10] R. J. Glauber, *Cross sections in deuterium at high energies*, *Phys. Rev.* **100** (Oct, 1955) 242–248.
- [11] R. J. Glauber, *Lectures in Theoretical Physics Volume 1*, .
- [12] FOR THE HALL A COLLABORATION collaboration, W. U. Boeglin, L. Coman, P. Ambrozewicz, K. Aniol, J. Arrington, G. Batigne et al., *Probing the high momentum component of the deuteron at high Q^2* , *Phys. Rev. Lett.* **107** (Dec, 2011) 262501.
- [13] CLAS COLLABORATION collaboration, K. S. Egiyan, G. Asryan, N. Gevorgyan, K. A. Griffioen, J. M. Laget, S. E. Kuhn et al., *Experimental Study of Exclusive $^2H(e, e'p)n$ Reaction Mechanisms at High Q^2* , *Phys. Rev. Lett.* **98** (Jun, 2007) 262502.
- [14] HALL C COLLABORATION collaboration, C. Yero, D. Abrams, Z. Ahmed, A. Ahmidouch, B. Aljawineh, S. Alsalmi et al., *Probing the deuteron at very large internal momenta*, *Phys. Rev. Lett.* **125** (Dec, 2020) 262501.

- [15] M. M. Sargsian and F. Vera, *New structure in the deuteron*, *Phys. Rev. Lett.* **130** (Mar, 2023) 112502.
- [16] F. Vera, *Probing the Structure of Deuteron at Very Short Distances*. Phd thesis, Florida International University, Miami, FL, July, 2021.
- [17] L. Frankfurt, M. Sargsian and M. Strikman, *Recent observation of short range nucleon correlations in nuclei and their implications for the structure of nuclei and neutron stars*, *Int. J. Mod. Phys. A* **23** (2008) 2991–3055, [0806.4412].
- [18] L. L. Frankfurt and M. I. Strikman, *Hard Nuclear Processes and Microscopic Nuclear Structure*, *Phys. Rept.* **160** (1988) 235–427.
- [19] M. Harvey, *Effective nuclear forces in the quark model with Delta and hidden color channel coupling*, *Nucl. Phys. A* **352** (1981) 326–342.
- [20] C.-R. Ji and S. J. Brodsky, *Quantum Chromodynamic Evolution of Six Quark States*, *Phys. Rev. D* **34** (1986) 1460.
- [21] J. Hockert, D. Riska, M. Gari and A. Huffman, *Meson exchange currents in deuteron electro-disintegration*, *Nuclear Physics A* **217** (1973) 14–28.
- [22] W. Fabian and H. Arenhovel, *Pion Exchange Currents and Isobar Configurations in Deuteron Electrodisintegration Below Pion Threshold*, *Nucl. Phys. A* **258** (1976) 461–479.
- [23] M. M. Sargsian, *Selected topics in high energy semiexclusive electronuclear reactions*, *Int. J. Mod. Phys. E* **10** (2001) 405–458, [nucl-th/0110053].
- [24] M. M. Sargsian et al., *Hadrons in the nuclear medium*, *J. Phys. G* **29** (2003) R1–R45, [nucl-th/0210025].
- [25] P. Stoler, *Baryon form factors at high q^2 and the transition to perturbative qcd*, *Physics Reports* **226** (1993) 103–171.
- [26] CLAS COLLABORATION collaboration, M. Ungaro, P. Stoler et al., *Measurement of the $n \rightarrow \Delta^+(1232)$ transition at high-momentum transfer by π^0 electroproduction*, *Phys. Rev. Lett.* **97** (Sep, 2006) 112003.
- [27] S. Jeschonnek and J. W. Van Orden, *Exclusive scattering from unpolarized and polarized deuteron*, *Few-Body Systems* **49** (Mar, 2011) 65–70.
- [28] W. P. Ford, S. Jeschonnek and J. W. Van Orden, *${}^2h(e, e' p)$ observables using a regge model parametrization of final-state interactions*, *Phys. Rev. C* **87** (May, 2013) 054006.
- [29] W. P. Ford, S. Jeschonnek and J. W. Van Orden, *Momentum distributions for ${}^2H(e, e' p)$* , *Phys. Rev. C* **90** (Dec, 2014) 064006.

- [30] A. Smith and S. Jeschonnek, *Relativistic Contributions to One-Body and Two-Body Electromagnetic Current Operators in $D(e,e'p)$ Reactions*, in *APS Division of Nuclear Physics Meeting Abstracts*, vol. 2021 of *APS Meeting Abstracts*, p. GA.019, Jan., 2021.
- [31] T. D. Forest, *Off-shell electron-nucleon cross sections: The impulse approximation*, *Nuclear Physics A* **392** (1983) 232–248.
- [32] W. U. Boeglin. Private communication, October, 2019.
- [33] C. Yero, *Cross Section Measurements of Deuteron Electro-Disintegration at Very High Recoil Momenta and Large 4-Momentum Transfers (Q^2)*. Phd thesis, Florida International University, Miami, FL, July, 2020.
- [34] L. L. Frankfurt, M. M. Sargsian and M. I. Strikman, *Feynman graphs and Gribov-Glauber approach to high-energy knockout processes*, *Phys. Rev. C* **56** (1997) 1124–1137, [[nucl-th/9603018](#)].

6 Appendix

6.1 PAC 52: LOI 12-24-005 || Reader Comments

The main goal of the LOI is to study the repulsive core of the short-range neutron-proton correlation inside deuterium. To this aim, the main problem is to find a kinematics where all other possible effects, in particular FSI, are suppressed.

Both theory expectations (Fig.1), previous experimental results (Fig.2), and your simulations of Fig.12 ([Fig.14 in PAC 53 proposal](#)) deliver the same message that the peak of FSI effects shifts to lower recoiling-neutron angles θ_{nq} at increasing missing momentum p_{miss} . The results in Fig.3 from previous Hall A experiment seem consistent: if the peak FSI shifts at lower θ_{nq} at larger p_{miss} , then the larger θ_{nq} the earlier (= the smaller p_{miss}) for the onset of FSI. Indeed, Fig.3 shows solid curves (FSI) that deviate from dashed ones (PWIA) for p_{miss} well below 700 MeV/c, even at 500 MeV/c at the largest angle (rightmost plot).

However, the puzzling feature of Fig.3 is that starting from some p_{miss} theory calculations (with or without FSI) start deviating from data. In the LOI, emphasis is put on the results for the CD Bonn optical potential, which deviate from data at very large $p_{miss} > 700$ - 800 MeV/c, depending on the angle. I understand that the reason for this emphasis is that at these p_{miss} there is the inelastic threshold of proton-neutron channel, opening up non-nucleonic degrees of freedom.

But results from other optical potential show very different deviations, even at p_{miss} as low as 500 MeV/c (green and blue curves in the leftmost plot). All the calculations (optical potential, off-shell electron-nucleon cross section in Eq.(4)) are all done in a non-relativistic framework, which is definitely not adequate for $p_{miss} \sim 800$ MeV/c which is the focus of the LOI. Moreover, relativistic corrections could heavily modify the simulations in Fig.12 ([Fig.14 in PAC 53 proposal](#)) for the largest p_{miss} values.

So, why invoking "exotic" effects (".. possible indication of the onset of non-nucleonic degrees of freedom...") before having all relativistic corrections under control?

I have also another question. In all previous experiments, and in the simulation discussed in Fig.12 ([Fig.14 in PAC 53 proposal](#)), there seems to be a specific angle, $\theta_{nq} \sim 40$ deg, at which FSI "switch off", irrespective of the kinematics explored (small or large p_{miss} , it does not matter). Since the indication instead is for a peak of FSI over PWIA shifting with p_{miss} , I'm wondering if there is any special reason for this 40 deg. angle. If there were one, it could solve the main problem raised in the LOI (= switch off FSI) without any additional measurement...

6.1.1 Question 1:

So, why invoking "exotic" effects (".. possible indication of the onset of non-nucleonic degrees of freedom...") before having all relativistic corrections under control?

Response:

We agree that one should expect significant relativistic effects for momenta above ~ 800 MeV/c, without attributing it to exotic non-nucleon component in the deuteron. However, as it was predicted in Ref. [15] the existence of non-nucleon components above the pn threshold will result in a violation of so-called "angular condition", in which case the extracted light-cone momentum distribution of the deuteron will depend on light cone momentum k and its transverse component k_\perp independently. Or in other words the non-polarized momentum distribution will depend on the direction of the internal momentum of the deuteron on the light-front. Even for the most relativistic case, if deuteron consists of proton and neutron only, the angular condition is satisfied and light-cone momentum distribution depends on the magnitude of k only. However, the existence of non-nucleonic component in the deuteron will result in an angular anisotropy [15]. Thus to obtain the signature of non-nucleon component the experiment needs to isolate the light-cone momentum distribution of the deuteron without effects of final-state interaction at different angles of recoil neutron. As a result, exploring the possible onset of non-nucleonic degrees of freedom in the deuteron requires a solid understanding of final-state interactions at bound nucleon momenta above ~ 800 MeV/c.

As such this proposal does **not** focus on searching for non-nucleonic components, but rather focuses on investigating the angular dependence of final-state interactions with θ_{nq} at momenta where non-nucleonic effects are expected to emerge in the ground state of deuteron wave function, i.e., ~ 800 MeV/c, (above the inelastic threshold of pn system) as there is currently **no** data that explores FSI in this region.

6.1.2 Question 2:

In all previous experiments, and in the simulation discussed in Fig.12([Fig.14 in PAC 53 proposal](#)), there seems to be a specific angle, $\theta_{nq} \sim 40$ deg, at which FSI "switch off", irrespective of the kinematics explored (small or large pmiss, it does not matter). Since the indication instead is for a peak of FSI over PWIA shifting with pmiss, I'm wondering if there is any special reason for this 40 deg. angle. If there were one, it could solve the main problem raised in the LOI (= switch off FSI) without any additional measurement...

Response:

Experimentally, there is **no** angle at which FSI are "turned off". The mention of a specific angle $\theta_{nq} \sim 40^\circ$ just refers the central value of a broader angular region at which FSI are suppressed. There are only certain angular regions in which FSI are the dominant contribution to the $d(e, e'p)n$ cross-section, and there are other regions in which FSI are suppressed, mainly at forward ($\theta_{nq} \lesssim 40^\circ$) and backward ($\theta_{nq} \gtrsim 120^\circ$) angles. At backward

angles, the kinematics are inelastic ($x_{Bj} < 1$) and intermediate nucleonic excitations like Isobar contributions contribute significantly to the cross-section, whereas at forward angles, $x_{Bj} > 1$, the PWIA becomes the dominant contribution to the $d(e, e'p)n$ cross-section.

The suppression of FSI at $\theta_{nq} \sim 40^\circ$ is due to cancellation of PWIA-FSI interference term with the $|FSI|^2$ term. This is a feature of eikonal (high energy) regime of FSI in which case pn rescattering amplitude is mainly imaginary and as a result Real part of the $iA_{FSI}A_{PWIA}$ interference term is negative, cancelling the $|A_{FSI}|^2$ term. As a result of this cancellation the cross section in this case is dominated by $|A_{PWIA}|^2$ term. This cancellation is in a fairly broad range of θ_{nq} and p_m . It was investigated in Ref. [1] within generalized eikonal approximation (GEA) and has been found that its position is defined by the average characteristics of the deuteron, pn re-scattering amplitude and kinetic energy of recoil particle. In the most simplified version (assuming single exponential form of the deuteron wave function) the cancellation happens at the transverse momentum of recoil nucleon:

$$p_{r\perp} \sim \sqrt{\frac{1}{\alpha_d} \ln \frac{32\pi\alpha_d}{\sigma_{pn}} + \frac{B_{pn}M_N^2}{2}\Delta^2},$$

where σ_{pn} is the total cross section of pn scattering, $\alpha_d = \frac{r_{rms}}{2p_{rms}}$, where r_{rms} and p_{rms} are RMS values of deuteron radius and internal momentum, B_{pn} is the exponent of the pn scattering amplitude presented in the diffractive form, M_N - is the mass of the nucleon, and $\Delta = \frac{q_0}{q}T_r$ where T_r , q_0 and q are the kinetic energy of the recoil nucleon, energy and momentum of the virtual photon respectively. Note that the Δ term accounts for the non-zero momentum of the scatterer in the deuteron which is not accounted in the standard Glauber approximation [34].

It is important to note that the angular dependence of the cross-sections on FSI has only been measured for recoil neutron momenta up to ~ 500 MeV/c [12], and predictions made about the suppression of FSI above ~ 500 MeV/c can be checked in the proposed experiment.